AD-A111 623 NEW MEXICO STATE UNIV LAS CRUCES DEPT OF PHYSICS F/G 7/4
HIGH RESOLUTION ATMOSPHERIC TRANSMITTANCE STUDY.(U)
JAN 82 R L ARMSTRONG DAAG29-77-G-0127

UNCLASSIFIED ARO-13746.1-GS NL

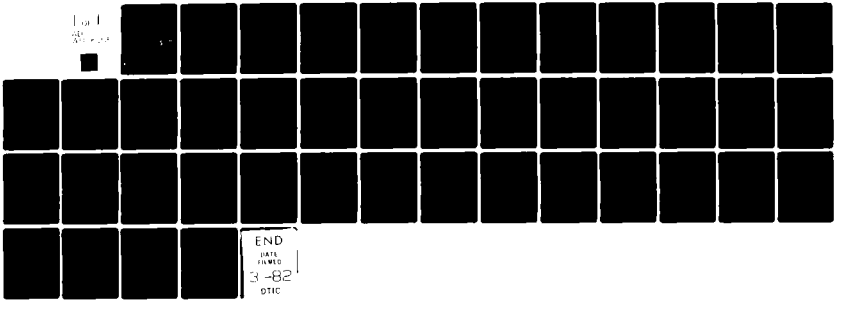

END
DATE FILMED
3-82
DTIC

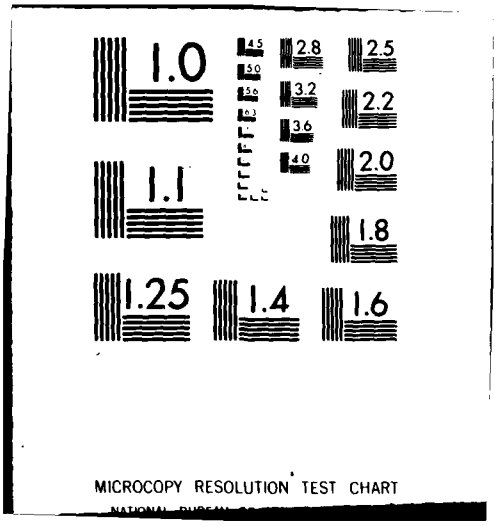
1.0
1.1
1.25
1.4
1.6
1.8
2.0
2.2
2.5
2.8
3.2
3.6
4.0
4.5
5.0
5.6
6.3
MICROCOPY RESOLUTION TEST CHART

SECURITY CLASSIFICATION OF THIS PAGE (When Data Entered)

REPORT DOCUMENTATION PAGE

BEFORE COMPLETING FORM

1. REPORT NUMBER: 13746.1-GS	2. GOVT ACCESSION NO. / 3. RECIPIENT'S CATALOG NUMBER
4. TITLE (and Subtitle): High Resolution Atmospheric Transmittance Study	5. TYPE OF REPORT & PERIOD COVERED: Final Report: 15 Apr 78 - 31 May 81
	6. PERFORMING ORG. REPORT NUMBER
7. AUTHOR(s): R. L. Armstrong	8. CONTRACT OR GRANT NUMBER(s): DAAG29 77 G 0127
9. PERFORMING ORGANIZATION NAME AND ADDRESS: New Mexico State University, Las Cruces, NM 88003	10. PROGRAM ELEMENT, PROJECT, TASK AREA & WORK UNIT NUMBERS
11. CONTROLLING OFFICE NAME AND ADDRESS: U. S. Army Research Office, Post Office Box 12211, Research Triangle Park, NC 27709	12. REPORT DATE: Jan 82 13. NUMBER OF PAGES: 40
14. MONITORING AGENCY NAME & ADDRESS(if different from Controlling Office)	15. SECURITY CLASS. (of this report): Unclassified 15a. DECLASSIFICATION/DOWNGRADING SCHEDULE

16. DISTRIBUTION STATEMENT (of this Report)

Approved for public release; distribution unlimited.

17. DISTRIBUTION STATEMENT (of the abstract entered in Block 20, if different from Report)

NA

18. SUPPLEMENTARY NOTES

The view, opinions, and/or findings contained in this report are those of the author(s) and should not be construed as an official Department of the Army position, policy, or decision, unless so designated by other documentation.

19. KEY WORDS (Continue on reverse side if necessary and identify by block number)

carbon dioxide
absorption spectra
infrared spectra
pressure effects
line mixing

20. ABSTRACT (Continue on reverse side if necessary and identify by block number)

A theoretical description of line mixing in the Q-branch of an infrared rotation-vibration band is obtained in the weak coupling approximation. The resulting absorption band shape is applied to the case of the ν_2-band of CO_2 near 667 cm^{-1}. Theoretical absorption profiles are illustrated in selected spectral regions for several values of the pressure.

DD FORM 1 JAN 73 1473 EDITION OF 1 NOV 65 IS OBSOLETE

UNCLASSIFIED

SECURITY CLASSIFICATION OF THIS PAGE (When Data Entered)

HIGH RESOLUTION ATMOSPHERIC TRANSMITTANCE STUDY

U.S. ARMY RESEARCH OFFICE GRANT NO. DAAG29-77-G-0127

Final Report

by

Robert L. Armstrong
Physics Department, New Mexico State University, Las Cruces, NM 88003

November 20, 1981

RESEARCH GRANT SUMMARY

Personnel

Dr. Robert L. Armstrong, Principal Investigator
Dr. Seung-yan Szeto, Post-doctoral Fellow
Mr. Glen H. Daw, Graduate Research Assistant

Reports and Publications

Progress Reports, periodically through duration of research effort
Final Report, this document
Research Paper, "Line Mixing in the ν_2-Band of CO_2," to be submitted for publication in Applied Optics

Objectives

The original objectives of this research project were:

1) to obtain experimental, high-resolution absorption spectra of CO_2 in the vicinity of the ν_2-band near 667 cm^{-1}.

2) to include line mixing effects into the theoretical description of the absorption spectrum.

In order to meet the first objective a tunable diode laser spectrometer was acquired from Laser Analytics, Inc. spectrometer was installed, aligned and calibrated. The necessary vacuum and gas-handling apparatus was constructed and tested to allow absorption spectra of research grade gaseous CO_2 to be taken at known pressures. In order to analyze the absorption spectra the experiment was placed on line to a PDP 11/60 computer located in an adjacent room in the physics building at New Mexico State

University. The necessary computer software was written to permit analysis of experimental absorption spectra. Preliminary absorption spectra were obtained for CO_2 at low pressures ~ 1 Torr (the Doppler-limited regime). Similar data had previously been reported by Aronson et al.[7] and has since been reported in a series of papers by Planet and Tettemer[8,9] (the reference numbers refer to the bibliography at the end of this report). The preliminary absorption spectra at low pressures were intended to serve as a calibration of the spectrometer resolution and sensitivity. The intention was to follow this preliminary series of low pressure experiments with experiments at higher pressures where line mixing effects could be studied. The results of the work described in this paragraph were reported to ARO in 4 Progress Reports covering the period April, 1977 - April, 1979.

At this point, as noted in a Progress Report sent to ARO in the fall of 1979, the laser diode failed. A replacement diode was ordered but difficulties in the fabrication of diodes at the desired frequency of 667 cm^{-1} resulted in an excessive delay before delivery of the diode. It was realized that alternative sources of diodes should be sought. One source was found, the Atmospheric Sciences Laboratory (ASL) at White Sands Missile Range. ASL kindly loaned us 3 diodes that covered the range from 950-1150 cm^{-1}. Since investigating the ν_2-band of CO_2 near 667 cm^{-1} was impossible with these diodes alternative spectral problems were considered. An initial group of candidates were the CO_2 laser bands at 950 and 1050 cm^{-1} but both preliminary absorption measurements and absorption calculations indicated that absorption from these bands was too weak to be detectable with our current spectrometer. The initial designs were being drawn for

a longer path length absorption cell, which would increase the sensitivity of our spectrometer, when the cryogenic compressor in the closed cycle helium refrigerator developed a vacuum leak. At this time the post-doctoral fellow, who had been working on the project with me, was forced by personal reasons to leave the project. I was able to hire a graduate student half-time for an entire academic year by using the remainder of the post-doctoral fellow's salary. The results of the efforts outlined in this paragraph we described in Progress Reports to ARO in the spring and fall of 1980, and the personnel action which resulted in the hiring of the graduate student was outlined in a letter to ARO in September of 1980.

Through the dilligent efforts of the graduate assistant the cryogenic compressor was placed back in working condition in the early spring of 1981. At this time extensive tests revealed the unfortunate fact that all diodes in our possession, the three diodes on loan from ASL and the replacement diode purchased over a year before, were either inoperative or had insufficient power levels for practical spectroscopic work. In particular the output power level of the 667 cm^{-1} diode was much too low to permit the higher pressure experiments to be done on the ν_2-band of CO_2. This unfortunate occurrence thus deprives this research effort from experimental data on the effect of line mixing in this theoretically and practically significant region of the spectrum.

The second objective of this research work has been achieved. A theoretical description of the absorption spectrum of the ν_2-band of CO_2

has been obtained which includes the effect of line mixing. The results of this work are given in the following report. An edited version of this report will be submitted shortly to Applied Optics for publication.

LINE MIXING IN THE ν_2-BAND OF CO_2*

by

R. L. Armstrong
Physics Department, New Mexico State University, Las Cruces, NM 88003

*This work supported by U.S. Army Research Office Grant No. DAAG29-77-G-0127.

ABSTRACT

A theoretical description of line mixing in the Q-branch of an infrared rotation-vibration band is obtained in the weak coupling approximation. The resulting absorption band shape is applied to the case of the ν_2-band of CO_2 near 667 cm^{-1}. Theoretical absorption profiles are illustrated in selected spectral regions for several values of the pressure.

I. Introduction

The determination of atmospheric absorption is important in the analysis of a variety of current scientific and technological problems as, for example, in the use of satellite-born infrared radiometers to retrieve atmospheric temperature profiles.[1,2] In the infrared region of the spectrum the shape of an absorption band is often modelled by summing the absorption at each frequency due to the individual lines in the band. Line parameter data is conveniently available for many molecules of atmospheric interest from the AFGL compilation.[3] The absorption profiles near line center are nearly Lorentzian at higher pressures: at lower pressures Doppler broadening effects are also significant.

The above approach is adequate at pressures where there is no appreciable overlap between lines in the absorption band. As the pressure is raised line mixing effects become significant and cause the absorption to depart from the summation over individual lines described above. Line mixing effects have been observed in infrared[4,5] and Raman spectra[6] at pressures in excess of one atmosphere. Other molecular systems, such as the Q-branches of infrared and Raman bands and the rotational Raman spectra of symmetric top or slightly asymmetric top molecules, have groups of overlapping lines even at the moderate pressures characteristic of the earth's atmosphere: line mixing should then be exhibited by these systems at pressures below one atmosphere.

In this paper we consider line mixing in the Q-branch of the ν_2-band of CO_2 near 667 cm^{-1}. This band is important in radiometric applications,[1,2] has been studied extensively at low pressures[7,8,9] and line parameter data are available from several sources.[3,7,8,9] The Q-branch consists of a series

of closely spaced lines, split by the rotation-vibration interaction. A qualitative interpretation of the pressure dependence of the Q-branch band shape may be given following the discussion of Alekseyev et al.[10] At low pressure, where the rotationally inelastic collision frequency is much less than the rotation-vibration interaction, the lines are well resolved: in this regime individual lines are broadened by collisions. As the pressure is increased the lines began to overlap and collisions broaden and mix the lines creating interference terms in the band shape. Finally, at high pressures, where the rotationally inelastic collision frequency is large compared to the rotation-vibration interaction, the lines in the band merge. In this regime modifications in the rotation-vibration interaction result in all lines in the band having the same vibration frequency: the band shape narrows with increasing pressure, producing the phenomenon of motional narrowing.[6] For the present case of the Q-branch of CO_2 we may obtain a measure of the rotation-vibration interaction by considering the line splitting in the neighborhood of the intensity maximum. These lines[3] are split by about .068 cm^{-1} and it may then be seen that, for T ~ 300 K, the rotationally inelastic collision frequency becomes equal to the rotation-vibration interaction at a pressure ~690 torr. Thus, line mixing should be significant in the Q-branch at pressures below one atmosphere but motional narrowing should not be significant until pressures of several atmospheres are reached.

The determination of the band shape in the presence of line mixing presumes a knowledge of the elements of the transition rate matrix.[11] Direct calculation of the elements of this matrix requires that, for an assumed inter-molecular potential, an average be taken over the dynamical variables describing a collision. This is a formidable numerical problem which, in

principle, must be solved for each value of temperature appropriate to the application. To circumvent this difficulty we assume in the remainder of this paper that the significant collisions which determine the band shape satisfy the weak coupling approximation.[12] In this approximation the rate matrix is dominated by its diagonal elements. In the present case we consider only the dominant isotopic species $^{12}C^{16}O_2$ for which symmetry considerations require J to be even. This implies that in most collisions the angular momentum either remains the same ($\Delta J = 0$) or changes at most by two units ($\Delta J = \pm 2$). The weak coupling approximation has been used by Rosenkranz[13] to adequately model the microwave spectrum of atmospheric oxygen near 5 mm. The work of Gordon and McGinnis[4] on the infrared spectrum of CO near 2150 cm^{-1} also indicates the dominance of the near-diagonal terms in the rate matrix.

II. Weak Coupling Approximation

In the Heisenberg picture of spectroscopy[14] the absorption band shape is determined by the Fourier transform of the transition dipole moment correlation function:

$$\langle \vec{\mu}(0) \cdot \vec{\mu}(t) \rangle = \mathbf{d} \cdot \exp[i(\omega_0 + i\Pi)] \cdot \rho \cdot \mathbf{d} \ , \qquad (1)$$

where d and ρ are vectors of intrinsic line amplitudes and fractional populations, respectively, ω_0 is a matrix of line frequencies and Π is the transition rate matrix. The brackets indicate a thermal average. Diagonal elements of the rate matrix, Π_{kk}, give the rate at which collisions transfer amplitude away from line k to all other lines in the spectrum while the off-diagonal elements, $\Pi_{\ell k}$, give minus the rate at which collisions transfer amplitude from line k to line ℓ. The rate matrix may be conveniently expressed

in terms of a cross section matrix σ as:

$$\Gamma = n\bar{v}\sigma \ , \tag{2}$$

where n is the absorber number density, and $\bar{v}$ is the average absorber-perturber relative speed. The cross section matrix has elements:

$$\sigma_{\ell k} = \frac{1}{\bar{v}} \int \langle v(\delta_{\ell k} - S_{\ell k}) \rangle 2\pi b db, \tag{3}$$

where b is the impact parameter and $S_{\ell k}$ is an element of the scattering matrix that gives the fractional amplitude transferred by a collision into line ℓ from a unit amplitude in line k before the collision.

Gordon[11] has developed a semi-classical description of molecular collisions in order to simplify the problem of the determination of the scattering matrix elements, $S_{\ell k}$. In this description the frequencies of the lines in the spectrum are assigned to appropriate classical rotation frequencies by means of the correspondence principle. Thus, for an infrared rotation-vibration band the P- and R-branch lines arise from rotation of the transition dipole moment, in opposite senses, at frequencies appropriate to the overall rotation of the molecule. The Q-branch lines, however, arise from quantum mechanical transitions between different vibrational angular momentum states. The corresponding classical rotational frequencies for the Q-branch lines are then much higher than those of the P and R-branch lines. This case, Hund's case (a), has been considered by Gordon[15] who finds that in the classical description collisions do not couple the Q-branch to either the P or the R-branches (the P and R-branches are collisionally coupled principally by the so-called "reorientation effect" which is responsible for the collapse of the whole band to a single line at extremely high pressures,

but this coupling does not concern us here). Thus, in the study of the Q-branch absorption we need consider only the effect of collisions that transfer amplitude between different Q-branch lines.

In the weak coupling approximation[13] the assumption is made that in most collisions the angular momentum either remains the same or changes at most by two units. Thus each column of the rate matrix contains: a) the diagonal element Π_{kk}; 2) an element Π_{k-2k} coupling line k to the adjacent line at lower frequency; and 3) an element Π_{k+2k} coupling line k to the adjacent line at higher frequency. Because of the definitions of the elements of the rate matrix, conservation of probability requires that each column satisfy:

$$\sum_{\ell} \Pi_{\ell k} = 0 \ , \tag{4}$$

which in the weak coupling approximation becomes:

$$\Pi_{k-2k} + \Pi_{kk} + \Pi_{k+2k} = 0 \ . \tag{5}$$

There is a second, rigorous, relationship between elements of the rate matrix required by the principle of detailed balance.[16] This requirement, which insures that the absorbing system remains in thermal equilibrium, results in elements of the rate matrix satisfying the relation:

$$\rho_k \ \Pi_{k-2k} = \rho_{k-2} \ \Pi_{kk-2} \ . \tag{6}$$

The diagonal elements of the rate matrix are simply the isolated linewidths and are available from several sources.[3,8,9] Equations (5) and (6) therefore suffice to determine all elements of the rate matrix in the weak coupling approximation.

Following Rosenkranz[13] we solve for the elements in descending order. The reason for this is that Eq. (5) is only an approximate relation, obtained by truncating Eq. (4), whereas Eq. (6) is exact. Thus, when we apply Eq. (5) to the highest frequency line considered we set $\Pi_{k+2k} = 0$ and introduce a large relative error into the values of the elements for that line. But, this error, and hence the error introduced into the rate matrix elements, is damped by successive applications of Eq. (6). Provided we select a maximum line frequency for which the Boltzmann factor is extremely small, the initial error will produce only a small effect in lines for which the population is large.

In the present case we have included lines up to J = 106; data for these lines are available from the AFGL compilation.[3] We thus set:

$$\Pi_{108,106} = 0 \ . \tag{7}$$

Application of Eqs. (5) and (6) then gives:

$$\Pi_{106-2(m+1),106-2m} = \sum_{\ell=0}^{m} (-1)^{\ell+1} \alpha_{106-2(m-\ell)} \frac{\rho_{106-2(m-\ell)}}{\rho_{106-2m}} \ , \tag{8}$$

where the linewidth $\alpha_m = \Pi_{mm}$ is the diagonal element for the m^{th} column of the rate matrix. Equation (5) may be used to generate the corresponding rate matrix elements coupling each line to the adjacent line at higher frequency, except for the lowest frequency, J = 2, line which must be handled separately. The reason for this is again the result of the approximate nature of Eq. (5). For the J = 2 line we must set $\Pi_{02} = 0$. In this case Eqs. (5) and (6) may not be satisfied simultaneously. We choose to satisfy the rigorous condition, Eq. (6), which in this case takes the form:

$$\rho_2 \Pi_{42} = \rho_4 \Pi_{24} \quad . \tag{9}$$

The approximate relation, Eq. (5), is then not satisfied for the lowest frequency line.

The absorption coefficient may be computed from the Fourier transform of the transition dipole correlation function, Eq. (1). The result is:

$$K(\omega) = \frac{8\pi^3 n\omega(1-e^{-hc\omega/kT})}{3hc} F(\omega) \quad , \tag{10}$$

where

$$F(\omega) = \frac{1}{\pi} \text{Im } d\cdot(\omega 1 - \omega_0 - i\Pi)^{-1}\cdot\rho\cdot d \quad , \tag{11}$$

with 1 the unit matrix. The formal mathematical problem in obtaining a solution to Eq. (11) is to diagonalize the non-Hermitian matrix $(\omega_0 + i\Pi)$. A generalized approach, the QR algorithm,[17] exists for performing this diagonalization, as well as an approximate perturbation theory solution. Following Rosenkranz[13] we elect to use the perturbation approach. It is shown in Appendix A that, to first-order in the elements $\Pi_{\ell k}$ (which is equivalent to a first-order expansion in the pressure), the eigenvalues of $(\omega_0 + i\Pi)$ are:

$$\lambda_k = \omega_k + i\alpha_k \quad , \tag{12}$$

while the eigenvectors have elements:

$$X_{\ell k} = 1 \quad , \quad \ell = k \tag{13a}$$

$$= i \frac{\Pi_{\ell k}}{\omega_k - \omega_\ell}, \quad \ell \neq k \tag{13b}$$

Then it may be shown, using Eqs. (6,12,13), that the following expression results for $F(\omega)$:

$$F(\omega) = \frac{1}{\pi} \sum_k \rho_k \frac{d_k d_k^2 + (\omega-\omega_k) y_k}{(\omega-\omega_k)^2 + \alpha_k^2} , \qquad (14)$$

where

$$y_k = 2d_k \sum_{\ell \neq k} \frac{d_\ell \Pi_{\ell k}}{\omega_k - \omega_\ell} . \qquad (15)$$

In the following section we will apply these results to the analysis of the Q-branch band shape.

Two approximations were made in the derivations of Eqs. (14) and (15); the weak-coupling approximation and the linear approximation to the eigenvalues and eigenvectors of the matrix $(\omega_0 + i\Pi)$. In order to disentangle the effects of these two approximations on the computed band shape in a simple case, we have considered a synthetic spectrum containing just 4 lines. Assuming the weak coupling approximation to be valid we have, with the aid of Eqs. (5) and (6), rigorously diagonalized the matrix $(\omega_0 + i\Pi)$. The details of this calculation are given in Appendix B. Although the synthetic 4-line spectrum is not equivalent to the Q-branch spectrum at elevated temperatures (e.g., at T ~ 300 K the maximum Q-branch intensity occurs for J = 16, the 8^{th} line in the band), at sufficiently low temperatures and pressures the synthetic spectrum will approximate the Q-branch spectrum. In the following section we investigate, for low temperatures and pressures, the correspondence between the synthetic 4-line spectrum and the spectrum obtained using eqs. (14) and (15), and hence get a measure of the validity of the linear approximation.

III. Absorption Band Shape

We consider the absorption coefficient $K(\omega)$, given by Eq. (10), where the spectral function $F(\omega)$ is given by Eqs. (14) and (15). The line amplitudes d_k may be expressed in terms of rotational line amplitudes D_k according to:[3]

$$d_k = (|\beta_v|^2)^{\frac{1}{2}} D_k \ , \tag{16}$$

where β_v is a reduced vibrational matrix element. It is convenient to define an integrated band intensity S_v^o by:[3]

$$S_v^o = \frac{32\pi^3 \ \omega_v(1-e^{-hc\omega_v/kT})}{3hc} \ |\beta_v|^2 \ , \tag{17}$$

where ω_v is the frequency of the band origin. Then in terms of S_v^o we may express the absorption coefficient, neglecting a small non-rigidity factor,[3] as:

$$K(\omega) = \frac{nS_v^o \ \omega(1-e^{-hc\omega/kT})}{\omega_v(1-e^{-hc\omega_v/kT})} \ G(\omega), \tag{18}$$

where the spectral function $G(\omega)$ is defined by:

$$G(\omega) = G_P(\omega) + G_R(\omega) + G_Q(\omega). \tag{19}$$

In Eq. (19) the spectral functions $G_P(\omega)$, $G_R(\omega)$ and $G_Q(\omega)$ are defined in terms of the rotational line line amplitudes D_k. For the case of the ν_2 band of CO_2 we have:[18]

$$D_k^P = \left[\frac{2(k-1)}{2k+1}\right]^{\frac{1}{2}} , \tag{20a}$$

$$D_k^R = \left[\frac{2(k+2)}{2k+1}\right]^{\frac{1}{2}} , \tag{20b}$$

$$D_k^Q = [2]^{\frac{1}{2}} . \tag{20c}$$

Then we have:

$$G_P(\omega) = \frac{1}{\pi} \sum_k \rho_k \left[\frac{k-1}{2(2k+1)}\right] \frac{\alpha_k}{(\omega-\omega_k)^2 + \alpha_k^2} , \tag{21a}$$

$$G_R(\omega) = \frac{1}{\pi} \sum_k \rho_k \left[\frac{k+2}{2(2k+2)}\right] \frac{\alpha_k}{(\omega-\omega_k)^2 + \alpha_k^2} , \tag{21b}$$

$$G_Q(\omega) = \frac{1}{2\pi} \sum_k \rho_k \frac{\alpha_k + (\omega-\omega_k)Y_k}{(\omega-\omega_k)^2 + \alpha_k^2} , \tag{21c}$$

where

$$Y_k = 2 \sum_{\ell \neq k} \frac{\Pi_{\ell k}}{\omega_k - \omega_\ell} . \tag{22}$$

Equation (18) for the absorption coefficient, together with the definitions of the spectral functions given by Eqs. (21a)-c) and (22), may then be used to compute an absorption band shape. The P and R-branch lines which overlap the Q-branch must be included in order to get a meaningful band shape, although there is no mixing between them. Figures 1-6 are plots of the computed absorption for two spectral regions; below the band origin from 661-667 cm^{-1}, and the region that includes the first 4 Q-branch lines from 667.366-667.469 cm^{-1}. Pressures of 10, 50, and 100 torr are considered, all for a temperature of 300 K.

The plots of the 661-667 cm^{-1} region illustrate the low frequency wing of the Q-branch including the first four P-branch lines. The solid curve is the

FIG. 1 Theoretical absorption coefficient versus frequency, 661-667 cm^{-1} region, ν_2-band of CO_2; pressure 10 Torr; temperature 300 K; solid curve with line mixing; unconnected points with no line mixing.

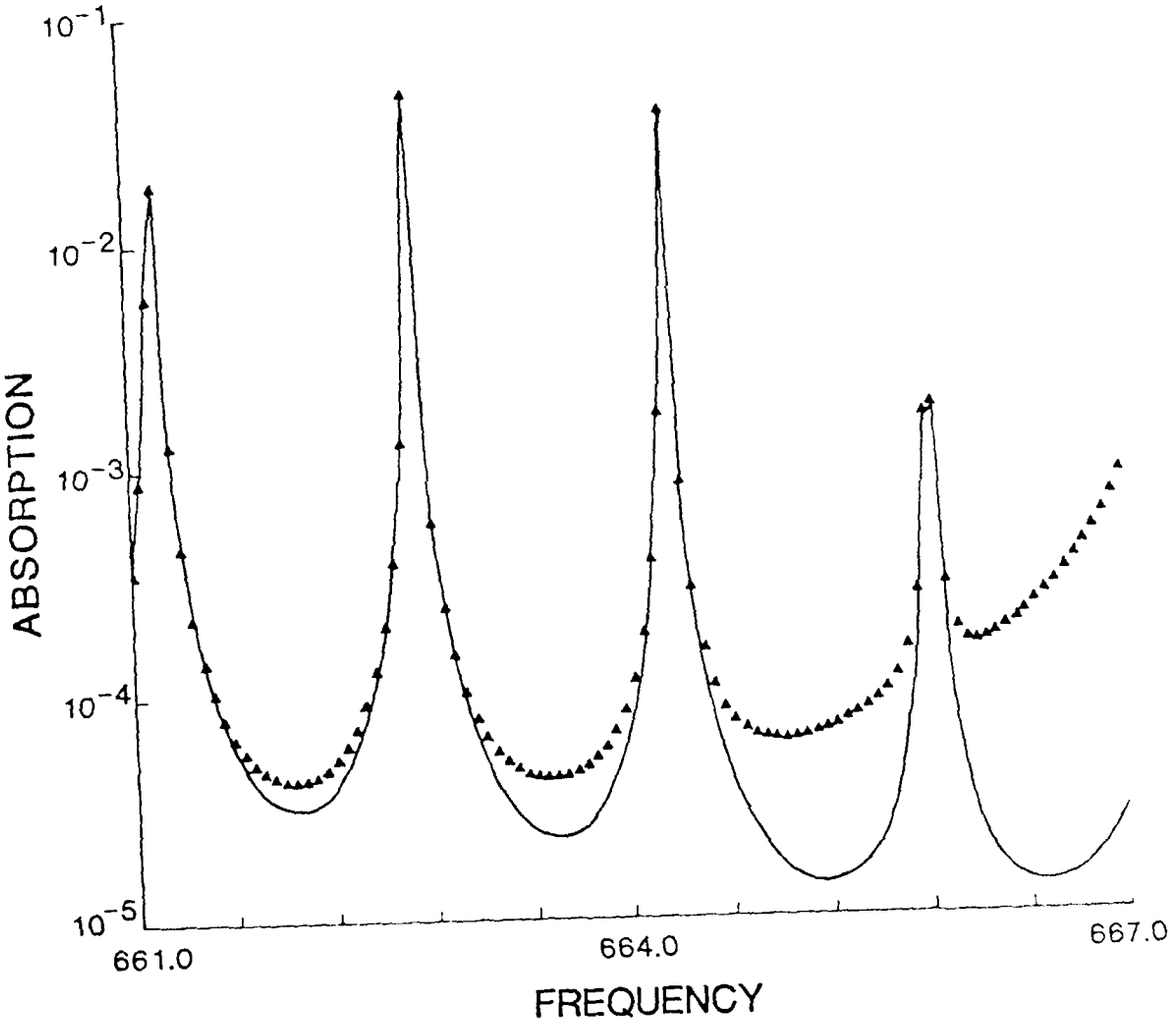
10^{-1}
10^{-2}
10^{-3}
10^{-4}
10^{-5}
ABSORPTION
661.0
664.0
667.0
FREQUENCY

FIG. 2 Theoretical absorption coefficient versus frequency, 661-667 cm^{-1} region, ν_2-band of CO_2; pressure 50 Torr; temperature 300 K; solid curve with line mixing; unconnected points with no line mixing.

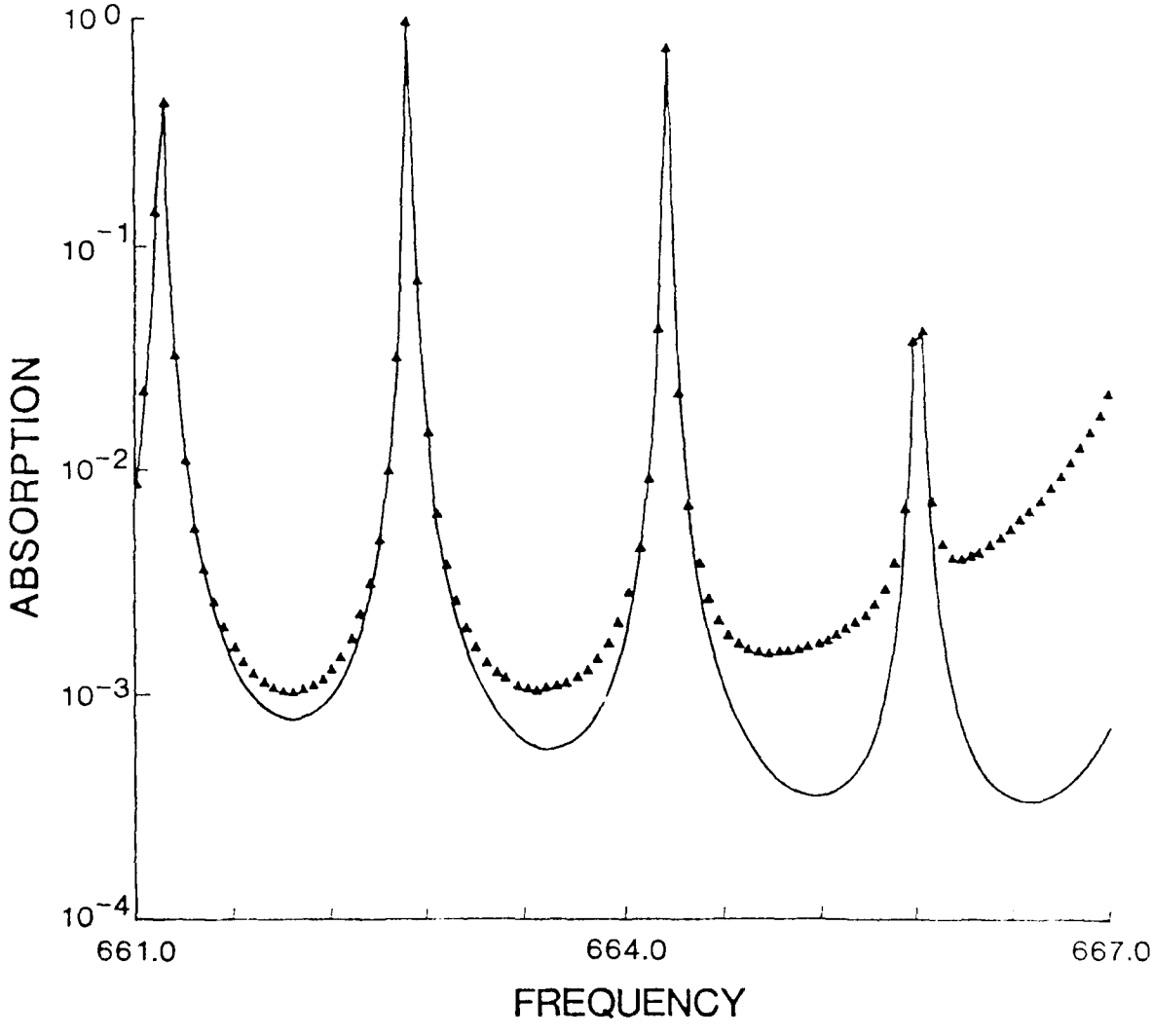
10 0
10 -1
10 -2
10 -3
10 -4
ABSORPTION
661.0
664.0
667.0
FREQUENCY

FIG. 3 Theoretical absorption coefficient versus frequency, 661-667 cm^{-1} region, ν_2-band of CO_2; pressure 100 Torr; temperature 300 K; solid curve with line mixing; unconnected points with no line mixing.

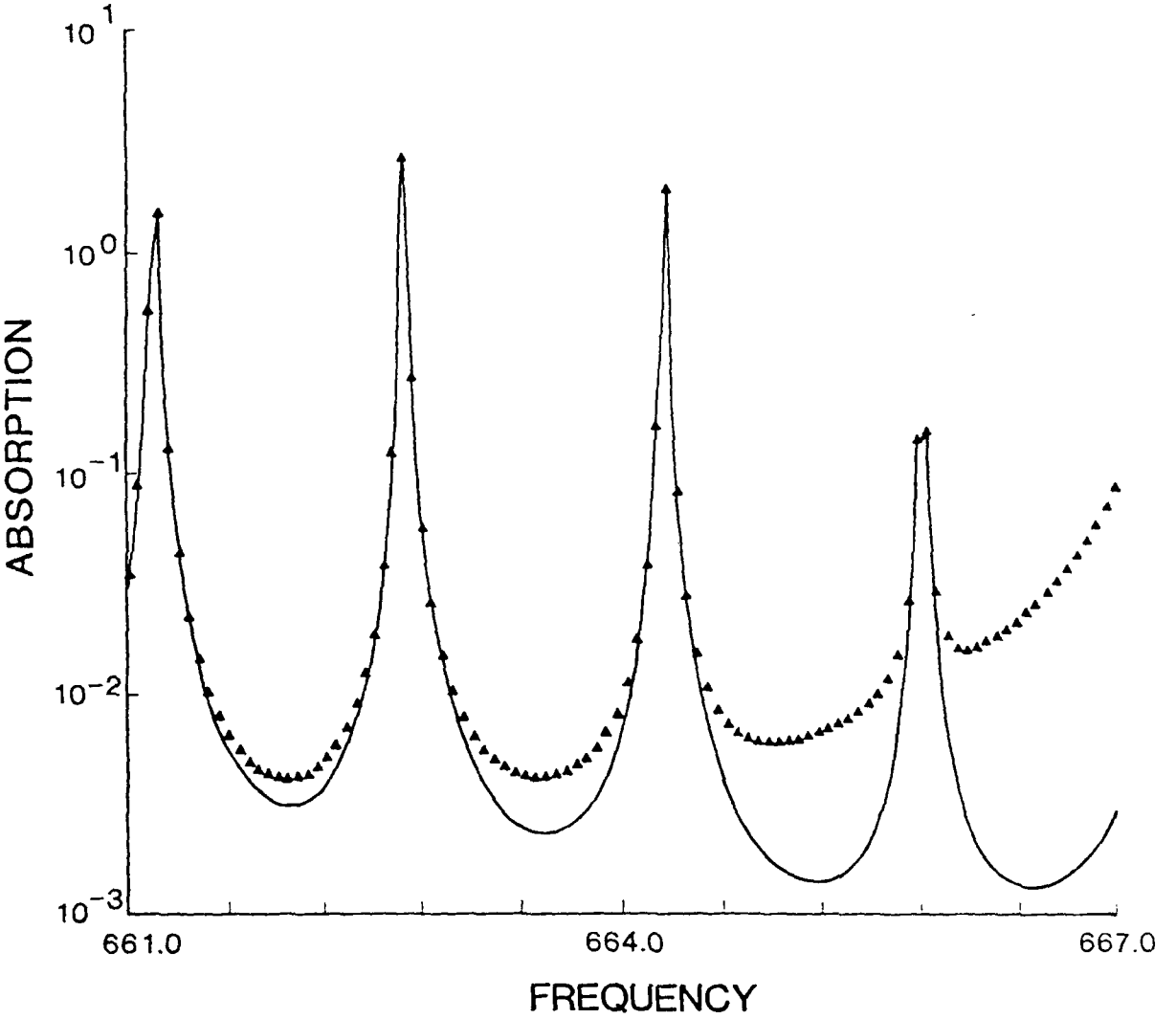
10^{1}
10^{0}
10^{-1}
10^{-2}
10^{-3}
ABSORPTION
661.0
664.0
667.0
FREQUENCY

FIG. 4 Theoretical absorption coefficient versus frequency, 667.366-667.469 cm^{-1} region, ν_2-band of CO_2; pressure 10 Torr; temperature 300 K; solid curve with line mixing; unconnected points with no line mixing.

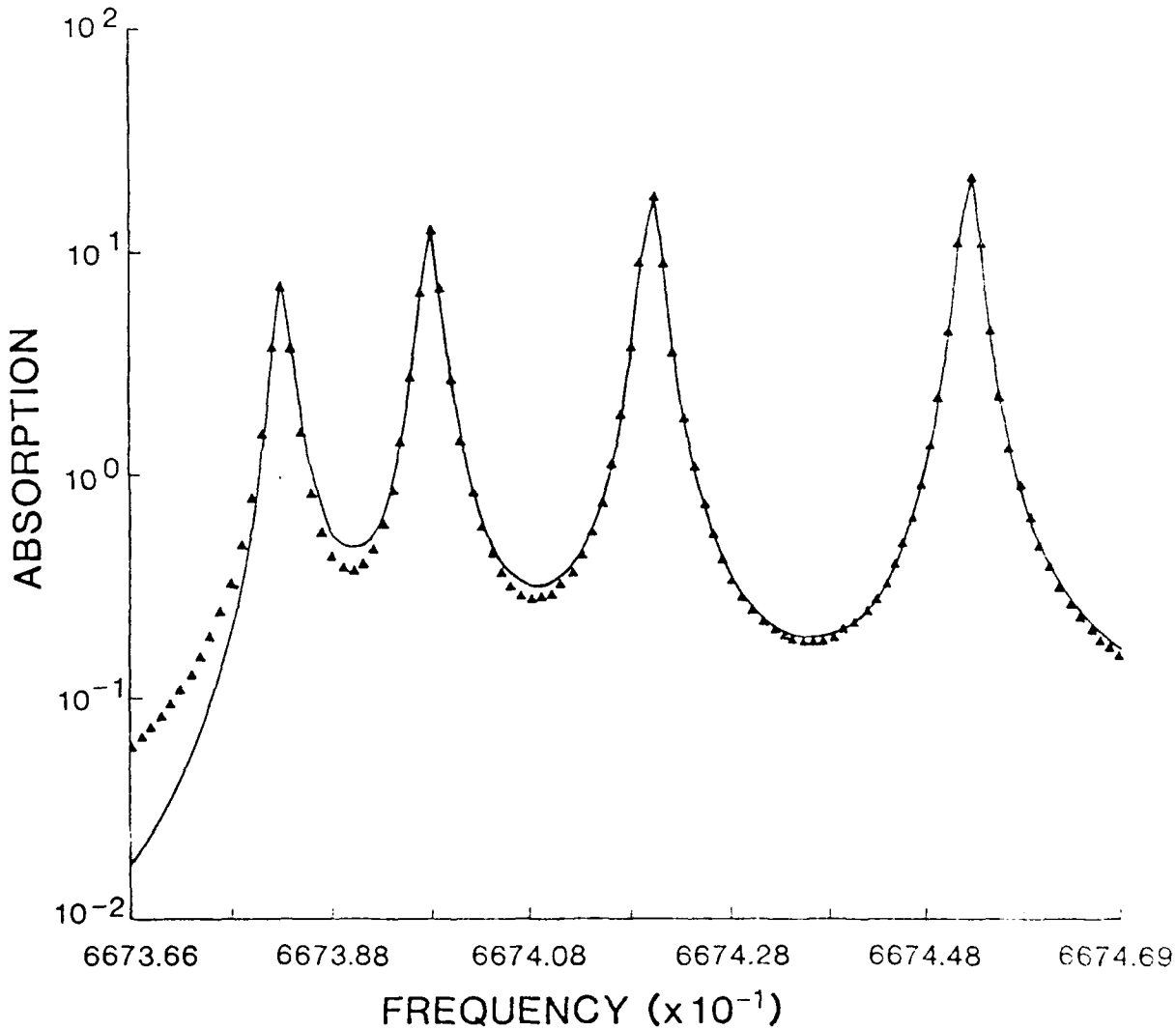
10^2
10^1
10^0
10^{-1}
10^{-2}
ABSORPTION
6673.66
6673.88
6674.08
6674.28
6674.48
6674.69
FREQUENCY ($\times 10^{-1}$)

FIG. 5 Theoretical absorption coefficient versus frequency, 667.366-667.469 cm^{-1} region, ν_2-band of CO_2; pressure 50 Torr; temperature 300 K; solid curve with line mixing; unconnected points with no line mixing.

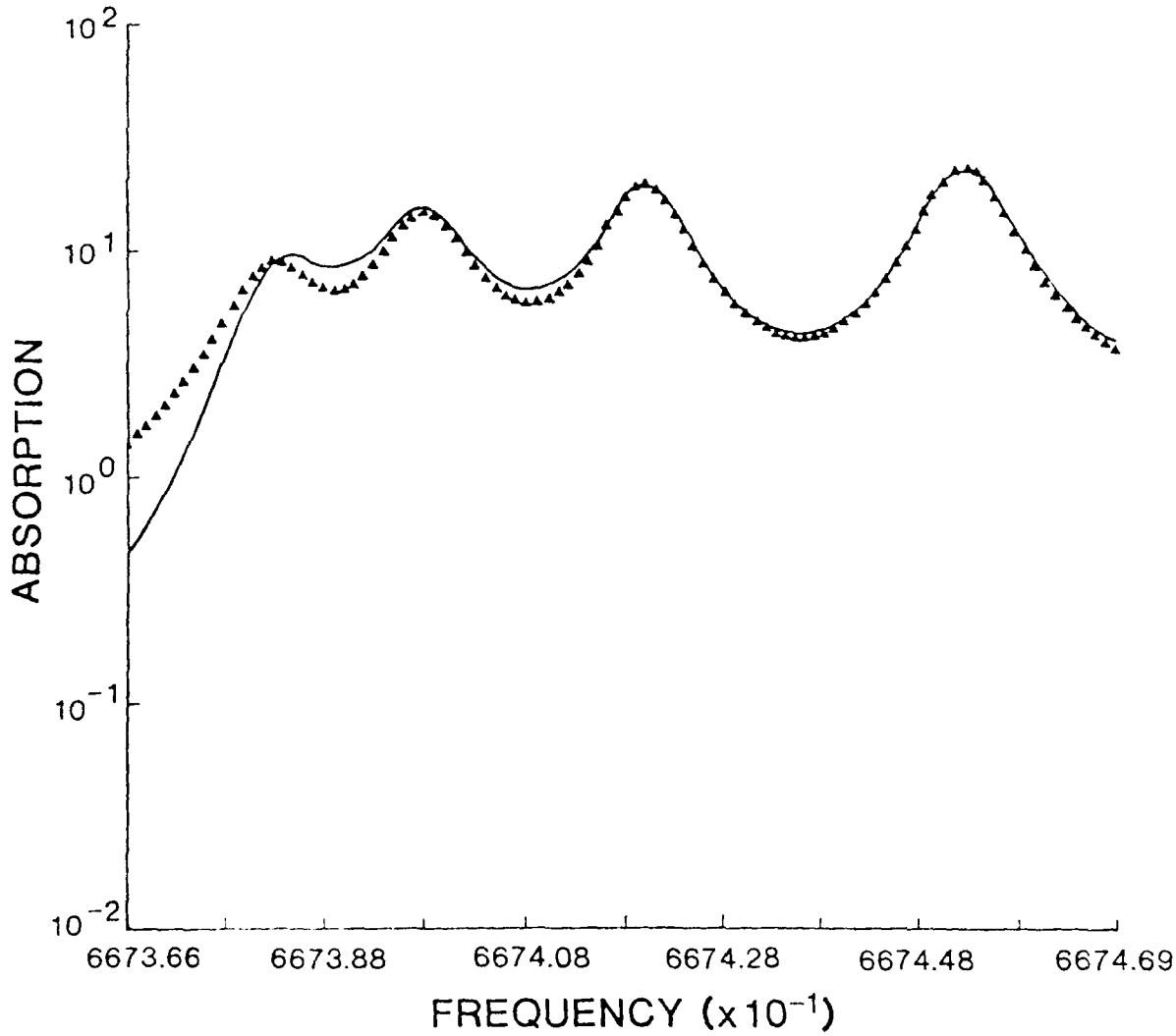
10^2
10^1
10^0
10^{-1}
10^{-2}
ABSORPTION
6673.66
6673.88
6674.08
6674.28
6674.48
6674.69
FREQUENCY ($\times 10^{-1}$)

FIG. 6 Theoretical absorption coefficient versus frequency, 667.366-667.469 cm^{-1} region, ν_2-band of CO_2; pressure 100 Torr; temperature 300 K; solid curve with line mixing; unconnected points with no line mixing.

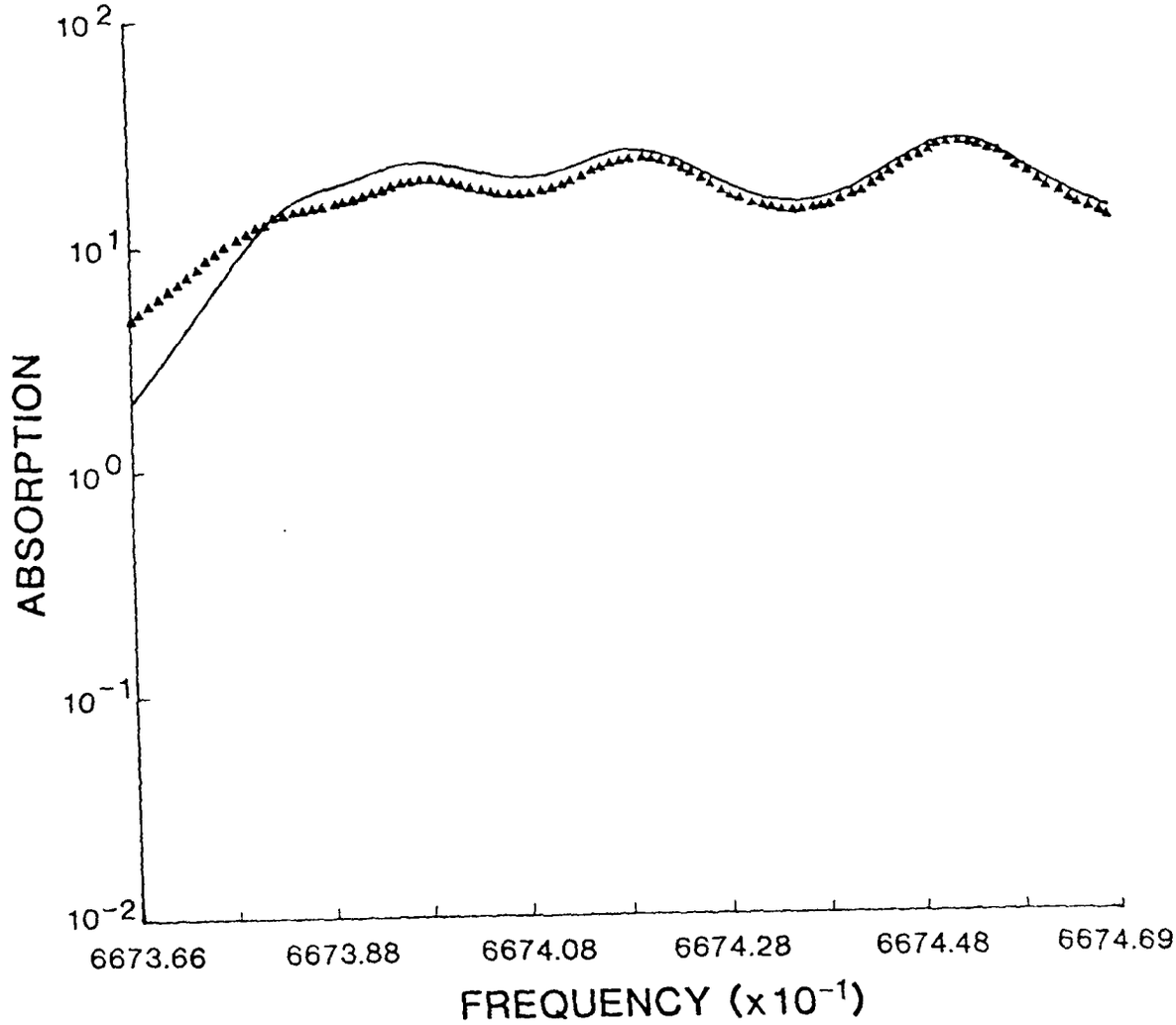
10^2
10^1
10^0
10^{-1}
10^{-2}
ABSORPTION
6673.66
6673.88
6674.08
6674.28
6674.48
6674.69
FREQUENCY ($\times 10^{-1}$)

computed absorption with line mixing included while the unconnected points illustrate the case of no line mixing (all $Y_k = 0$ in Eq. (22)). The effect of line mixing is seen to be most apparent in the troughs between the P-branch lines, reducing the absorption there by greater than a factor of 10 just below the band origin at 667 cm^{-1}. The effect of line mixing is also observed to be linearly dependent on pressure in the troughs, appropriate to the first-order approximation made in inverting the matrix $(\omega_0 + i\Gamma)$. Truncation of the P_2 line is caused by a lack of resolution in the plotting program.

The plots of the spectral region near 667 cm^{-1} illustrate the dependence of the line mixing effect on the splitting of the lines.[10] The rotation-vibration interaction results in an increased line splitting with increasing J, with the smallest splitting, .015 cm^{-1}, occurring between the lowest members of the Q-branch, Q_2 and Q_4. The effect of line mixing should then be first evident in the lowest Q-branch lines, progressing with increasing pressure to higher Q-branch lines. This is clearly shown in Figs. 4-6. At the lowest pressure of 10 torr line mixing has already reduced the absorption a factor ~2 below Q_2, whereas the absorption near Q_8 remains virtually unaffected. At the higher pressures of 50 and 100 torr line mixing is seen to have a progressively greater effect on the higher Q-branch lines.

Figure 7 illustrates the effect of the linear pressure approximation made in obtaining the eigenvalues and eigenvectors of the matrix $(\omega_0 + i\Gamma)$. The solid line gives the calculated absorption for a synthetic 4-line Q-branch. The weak-coupling approximation was used to compute this spectrum but the matrix $(\omega_0 + i\Gamma)$, as shown in Appendix B, was rigorously diagonalized. The unconnected points represent the calculated absorption in the linear pressure approximation. The synthetic 4-line spectrum does not closely approximate

FIG. 7 Synthetic absorption coefficient versus frequency, 667.366-667.469 cm^{-1} region, ν_2-band of CO_2; pressure 10 Torr, temperature 25 K; solid curve, exact 4-line spectrum; unconnected points, linear pressure approximation.

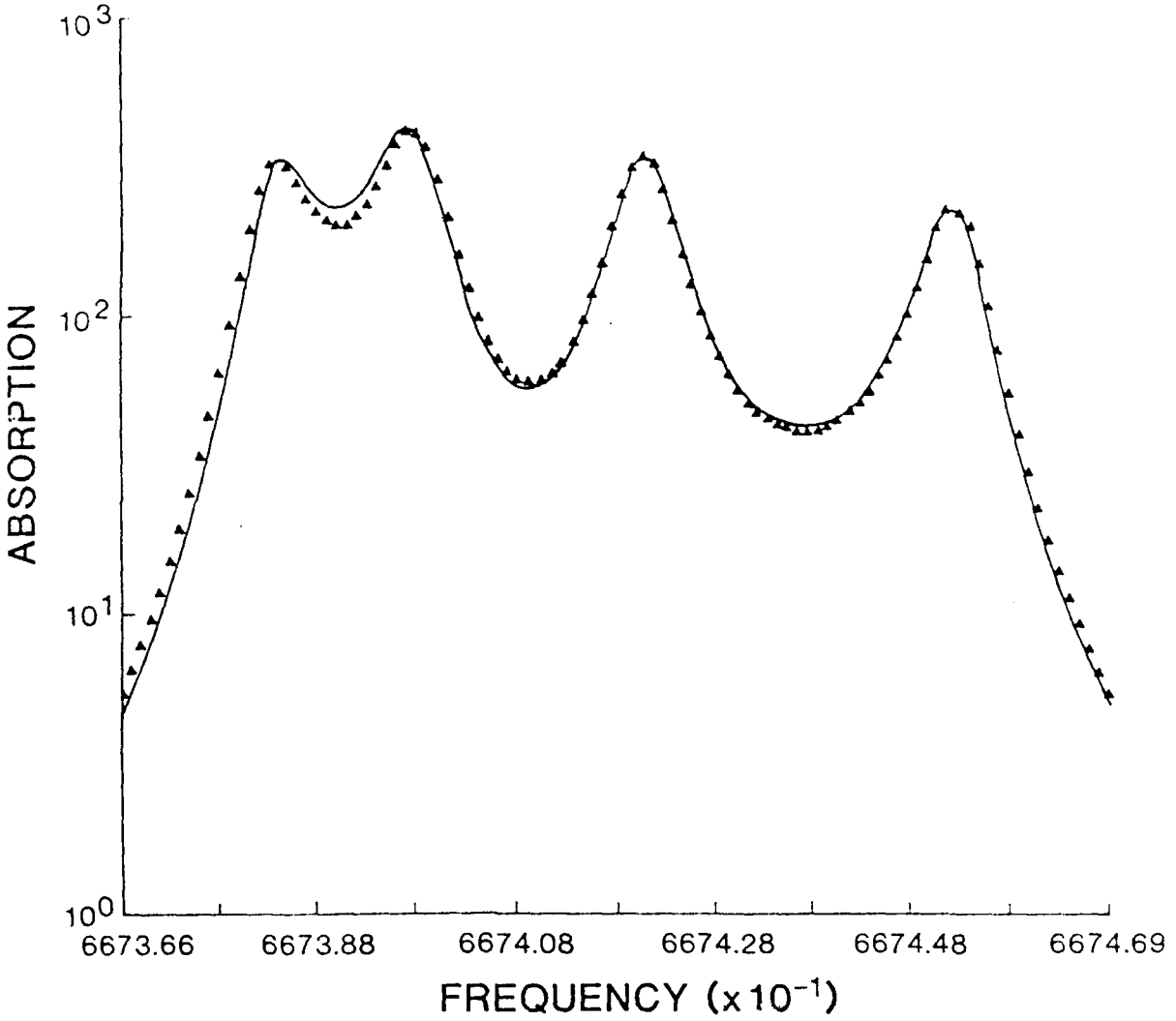
10^3
10^2
10^1
10^0
ABSORPTION
6673.66
6673.88
6674.08
6674.28
6674.48
6674.69
FREQUENCY ($\times 10^{-1}$)

the Q-branch at elevated temperatures but at sufficiently low temperatures the population of the rotational levels falls off quickly and the synthetic four-line spectrum becomes an increasingly useful approximation. Figure 7 illustrates the case of T = 25 K, for which the peak population occurs for the Q_4 line (note that this represents a "non-physical" case since gaseous CO_2 could not exist at this temperature in thermal equilibrium. The purpose here, however, is simply to compare two theoretical descriptions of the absorption, and the non-physical nature of the temperature is of no significance). The major discrepancy occurs in the vicinity of the Q_2 line, below line center, and in the trough between the Q_2 and Q_4 lines, reaching a maximum value of about 20% there. In the remainder of the spectral region the two computed spectra are virtually indistinguishable. A comparison of Fig. 7 with Figs. 1-6 reveals that the exact calculated *absorption* enhances the effect of line mixing as compared with the linear approximation. For example, below the center of the Q_2 line, the exact *absorption* falls below the linear result, whereas in the trough between the Q_2 and Q_4 lines the exact absorption results in the depth of the trough being reduced further than is predicted by the linear theory. We conclude that the effect of line mixing will be at least as large as the prediction of the linear pressure theory.

IV. Conclusions and Recommendations

In this report we have computed the effect of line mixing on the Q-branch of the ν_2-band of CO_2 near 667 cm^{-1}. The weak coupling approximation was used to generate the elements of the transition rate matrix. The spectrum was computed by means of a linear approximation, which was used to diagonalize the matrix $(\omega_0 + i\Pi)$. Absorption band shapes were computed for two spectral

regions, below the band origin from 661-667 cm^{-1} and in the region of the first 4 Q-branch lines above 667 cm^{-1}. Finally, the absorption spectrum using the linear approximation was compared with a synthetic spectrum in which the matrix $(\omega_0 + i\Pi)$ was rigorously diagonalized.

In the linear pressure approximation line mixing is seen from Figs. 1-6 to have a significant effect on the computed spectrum. For the pressures considered, between 10 and 100 torr, the effect of line mixing is largest in the region just below the band origin near 667 cm^{-1} and in the troughs between the lowest Q-branch lines, around 667.4 cm^{-1}. We may conclude from the results illustrated in Fig. 7 that an exact weak coupling calculation of the absorption band shape would show line mixing effects at least as great as those shown in Figs. 1-6 computed using the linear approximation.

Several areas of additional research are suggested by the results of this study. First, the multi-line Q-branch spectrum should be rigorously diagonalized in the weak-coupling approximation. This is a difficult numerical problem but the QR algorithm[17], or its equivalent, could be used to obtain the spectrum. Second, experimental absorption spectra of CO_2 are needed at pressures above 10 torr where, from the results of this work, line mixing effects should be observable. It would, of course, also be of interest to extend the measurements to pressures of several atmospheres where motional narrowing should be observed. Finally, the validity of the weak coupling approximation for CO_2 has not been tested by the present work. A detailed calculation of the absorption band shape is clearly needed in which elements of the cross section matrix, given by Eq. (3), are computed directly from the collision dynamics.

REFERENCES

1. H. E. Fleming and W. L. Smith, Temperature, its Measurement and Control in Science and Industry (ed. by H. W. Plumb), vol. 4, part 3, pp. 2239-2250, Instrument Society of America, Pittsburgh, 1972.
2. S. Fritz, D. Q. Wark, H. E. Fleming, W. L. Smith, H. Jacobowitz, D. T. Hilleary and J. C. Alishouse, Temperature Sounding from Satellites, NOAA Technical Report NESS 59, U.S. Department of Commerce, Washington, D.C., July, 1972.
3. R. A. McClatchey, W. S. Benedict, S. A. Clough, D. E. Burch, R. F. Calfee, K. Fox, L. S. Rothman and J. S. Garing, AFCRL Atmospheric Absorption Line Parameters, AFCRL-TR-73-0006, 1973.
4. R. G. Gordon and R. P. McGinnis, J. Chem. Phys. 55, 4898 (1971).
5. A. Lightman and A. Ben-Reuven, J. Chem. Phys. 50, 351 (1969).
6. P. Dion and A. D. May, Can. J. Phys. 51, 36 (1973).
7. J. R. Aronson, P. C. von Thüna and J. F. Butler, Appl. Opt. 14, 1120 (1975).
8. W. G. Planet and G. L. Tettemer, J. Quant. Spectrosc. Radiat. Transfer 22, 345 (1979).
9. G. L. Tettemer and W. G. Planet, J. Quant. Spectrosc. Radiat. Transfer 24, 343 (1980).
10. V. Alekseyev, A. Grasiuk, V. Ragulsky, I. Sobel'man and F. Faizulov, IEEE J. Quantum Electron. QE-4, 654 (1968).
11. R. G. Gordon, J. Chem. Phys. 45, 1649 (1966).
12. W. A. Lester and R. B. Bernstein, J. Chem. Phys. 53, 11 (1970).

13. P. W. Rosenkranz, IEEE Trans. Antennas Propagat. AP-23, 498 (1975).

14. R. G. Gordon, J. Chem. Phys. 43, 1307 (1965).

15. R. G. Gordon, J. Chem. Phys. 46, 448 (1967).

16. D. L. Huber and J. H. Van Vleck, Rev. Mod. Phys. 49, 939 (1977).

17. J. H. Wilkinson, The Algebraic Eigenvalue Problem, Oxford Univ. Press, 1965.

18. G. Herzberg, Infrared and Raman Spectra, D. Van Nostrand Company, New York, 1945.

Appendix A. Perturbation Theory Calculation of Eigenvalues and Eigenvectors of the Matrix $(\omega_0 + i\Gamma)$

Consider the eigenvalue equation:

$$(A + \varepsilon B)x = \lambda x \ , \tag{A.1}$$

where ε is a smallness parameter. We expand the eigenvalues and eigenvectors in a power series in ε and collect terms proportional to each power. To second order:

$$Ax^{(0)} = \lambda^{(0)}x^{(0)} \ , \tag{A.2}$$

$$Ax^{(1)} + Bx^{(0)} = \lambda^{(0)}x^{(1)} + \lambda^{(1)}x^{(0)} \ , \tag{A.3}$$

$$Ax^{(2)} + Bx^{(1)} = \lambda^{(0)}x^{(2)} + \lambda^{(1)}x^{(1)} + \lambda^{(2)}x^{(0)} \ . \tag{A.4}$$

We assume in what follows that the eigenvalues $\lambda_k^{(0)}$ are non-degenerate and the corresponding eigenvectors $x_k^{(0)}$ are orthogonal and normalized so that:

$$x_\ell^{(0)} \cdot x_k^{(k)} = \delta_{\ell k} \tag{A.5}$$

we then expand $x_k^{(1)}$ in terms of the $x_\ell^{(0)}$:

$$x_k^{(1)} = \sum_\ell a_{\ell k}^{(1)} \, x_\ell^{(0)} \ , \tag{A.6}$$

and it may be shown that the first order corrections to the eigenvalue and eigenvector are:

$$\lambda_k^{(1)} = B_{kk} \ , \tag{A.7}$$

$$a_{\ell k}^{(1)} = \frac{B_{\ell k}}{\lambda_k^{(0)} - \lambda_\ell^{(0)}} \quad , \quad \ell \neq k . \tag{A.8}$$

Similarly, we expand $x_k^{(2)}$ in terms of the $x_\ell^{(0)}$:

$$x_k^{(2)} = \sum_\ell a_{\ell k}^{(2)} \, x_\ell^{(0)} \ , \tag{A.9}$$

and it may be shown that the second order corrections to the eigenvalue and eigenvector are:

$$\lambda_k^{(2)} = \sum_{\ell \neq k} \frac{B_{k\ell} \, B_{\ell k}}{\lambda_k^{(0)} - \lambda_\ell^{(0)}} \ , \tag{A.10}$$

$$a_{\ell k}^{(2)} = \sum_{m \neq k} \frac{B_{\ell m} \, B_{mk}}{(\lambda_k^{(0)} - \lambda_\ell^{(0)})(\lambda_k^{(0)} - \lambda_m^{(0)})} \ . \tag{A.11}$$

In our case we define:

$$A_{\ell k} = (\omega_k + i\alpha_k)\delta_{\ell k} \ , \tag{A.12}$$

$$B_{\ell k} = i\Pi_{\ell k} \quad , \quad \ell \neq k \tag{A.13}$$

$$= 0 \quad , \quad \ell = k .$$

Then to second order we get the eigenvalues and eigenvectors:

$$\lambda_k^{(0)} = \omega_k + i\alpha_k \ , \tag{A.14}$$

$$\lambda_k^{(1)} = 0, \tag{A.15}$$

$$\lambda_k^{(2)} = - \sum_{\ell \neq k} \frac{\Pi_{k\ell} \Pi_{\ell k}}{\omega_k - \omega_\ell} \ , \tag{A.16}$$

$$x_{\ell k}^{(0)} = \delta_{\ell k} \ , \tag{A.17}$$

$$x_{\ell k}^{(1)} = i \frac{\Pi_{\ell k}}{\omega_k - \omega_\ell} \ , \quad \ell \neq k \tag{A.18}$$

$$x_{\ell k}^{(2)} = - \sum_{m \neq k} \frac{\Pi_{\ell m} \Pi_{mk}}{(\omega_k - \omega_\ell)(\omega_k - \omega_m)} \ , \quad \ell \neq k \tag{A.19}$$

where in computing $\lambda_k^{(0)} - \lambda_\ell^{(0)} = \omega_k - \omega_\ell + i(\alpha_k - \alpha_\ell)$ we have neglected the imaginary term since the linewidths of adjacent lines are nearly identical.

Appendix B. Weak Coupling Calculation of a Four Line Spectrum

We wish to compute the absorption band shape, $F(\omega)$, given by Eq. (11) as:

$$F(\omega) = \frac{1}{\pi} \mathrm{Im}\, d\cdot(\omega 1 - \omega_0 - i\Pi)^{-1}\cdot\rho\cdot d \ . \tag{B.1}$$

From Eqs. (16) and (20c), we have for Q-branch lines:

$$F(\omega) = \frac{2}{\pi} |\beta_v|^2 \ H(\omega), \tag{B.2}$$

where

$$H(\omega) = \mathrm{Im}(\omega 1 - \omega_0 - i\Pi)^{-1}\cdot\rho \ . \tag{B.3}$$

The formal problem is then to obtain the inverse of the matrix:

$$M = (\omega 1 - \omega_0 - i\Pi). \tag{B.4}$$

In the weak-coupling approximation M contains only diagonal and 1st off-diagonal terms. It thus has the form:

$$M = \begin{bmatrix} m_{11} & m_{12} & 0 & 0 \\ m_{21} & m_{22} & m_{23} & 0 \\ 0 & m_{32} & m_{33} & m_{34} \\ 0 & 0 & m_{43} & m_{44} \end{bmatrix} . \tag{B.5}$$

The inverse is

$$M^{-1} = (\det M)^{-1} \tilde{M} \ , \tag{B.6}$$

where

$$\det M = b_1 b_2 - m_{11} m_{44} m_{23} m_{32}, \tag{B.7}$$

$$\tilde{M} = \begin{bmatrix} m_{22}b_2 - m_{23}m_{32}m_{44} & -m_{12}b_2 & m_{12}m_{23}m_{44} & -m_{12}m_{23}m_{34} \\ -m_{21}b_2 & m_{11}b_2 & -m_{23}m_{11}m_{44} & m_{11}m_{23}m_{34} \\ m_{32}m_{21}m_{44} & -m_{32}m_{11}m_{44} & m_{44}b_1 & -m_{34}b_1 \\ -m_{43}m_{32}m_{21} & m_{11}m_{43}m_{32} & -m_{43}b_1 & m_{33}b_1 - m_{23}m_{32}m_{11} \end{bmatrix} \tag{B.8}$$

In Eqs. (B.7), (B.8) we have used the abbreviations:

$$b_1 = m_{11}m_{22} - m_{12}m_{21} , \tag{B.9}$$

$$b_2 = m_{33}m_{44} - m_{34}m_{43} . \tag{B.10}$$

We then define the following quantities:

$$X_k = \omega - \omega_k , \tag{B.11}$$

$$Y_{\ell k} = X_\ell X_k - \alpha_\ell \alpha_k , \tag{B.12}$$

$$L_{\ell k} = X_\ell \alpha_k + X_k \alpha_\ell , \tag{B.13}$$

$$Z_{\ell k} = Y_{\ell k} + \Pi_{\ell k}\Pi_{k\ell} , \tag{B.14}$$

in terms of which we may express the real and imaginary parts of detM and $\tilde{M}$:

$$\det M = D' - iD'', \tag{B.15}$$

$$\tilde{M} = \tilde{M}' - i\tilde{M}'', \tag{B.16}$$

in the form:

$$D' = Z_{12}Z_{34} + Y_{14}\Pi_{23}\Pi_{32} - L_{12}L_{34} \ , \tag{B.17}$$

$$D'' = Z_{12}L_{34} + Z_{34}L_{12} + L_{14}\Pi_{23}\Pi_{32} \ , \tag{B.18}$$

$$\tilde{M}' = \begin{bmatrix} X_2Z_{34}-\alpha_2L_{34}+\Pi_{23}\Pi_{32}X_4 & \Pi_{12}L_{34} & -\Pi_{12}\Pi_{23}X_4 & 0 \\ \Pi_{21}L_{34} & X_1Z_{34}-\alpha_1L_{34} & \Pi_{23}L_{14} & -\Pi_{23}\Pi_{34}X_1 \\ -\Pi_{32}\Pi_{21}X_4 & \Pi_{32}L_{14} & X_4Z_{12}-\alpha_4L_{12} & \Pi_{34}L_{12} \\ 0 & -\Pi_{43}\Pi_{32}X_1 & \Pi_{43}L_{12} & X_3Z_{12}-\alpha_3L_{12} \\ & & & +\Pi_{23}\Pi_{32}X_1 \end{bmatrix} \tag{B.19}$$

$$\tilde{M}' = \begin{bmatrix} X_2L_{34}+\alpha_2Z_{34} & -\Pi_{12}Z_{34} & -\Pi_{12}\Pi_{23}\alpha_4 & \Pi_{12}\Pi_{23}\Pi_{34} \\ +\alpha_4\Pi_{23}\Pi_{32} & & & \\ -\Pi_{21}Z_{34} & \alpha_1Z_{34}+X_1L_{34} & -\Pi_{23}Y_{14} & -\Pi_{23}\Pi_{34}\alpha_1 \\ -\Pi_{32}\Pi_{21}\alpha_4 & -\Pi_{32}Y_{14} & \alpha_4Z_{12}+X_4L_{12} & -\Pi_{34}Z_{12} \\ \Pi_{43}\Pi_{32}\Pi_{21} & -\Pi_{43}\Pi_{32}\alpha_1 & -\Pi_{43}Z_{12} & X_3L_{12}+\alpha_3Z_{12} \\ & & & +\alpha_1\Pi_{23}\Pi_{32} \end{bmatrix}$$

In terms of these quantities the spectral function $H(\omega)$ may be written in the form:

$$H(\omega) = (D'^2 + D''^2)^{-1} \sum_{k=1}^{4} \theta_k [D''S_k' - D'S_k''], \tag{B.21}$$

where:

$$S_k' = \sum_{\ell=1}^{4} \tilde{M}'_{\ell k} , \tag{B.22}$$

$$S_k'' = \sum_{\ell=1}^{4} \tilde{M}''_{\ell k} . \tag{B.23}$$

The absorption coefficient for the synthetic 4-line Q-branch is then obtained by replacing $G_Q(\omega)$ in Eq. (21c) by:

$$G_Q(\omega) \rightarrow \frac{1}{2\pi} H(\omega). \tag{B.24}$$